



**HAL**  
open science

## 2-Azahetaryl-2-(oxoindolin-2-ylidene)acetonitriles as Colorimetric Probes for Zn: Synthesis and Optical Properties

Vladyslav V. Shcherban, Olena Kuleshova, Tetiana Ye. Keda, Olga V. Khilya,  
Emmanuel Gras, Yulian M. Volovenko

► **To cite this version:**

Vladyslav V. Shcherban, Olena Kuleshova, Tetiana Ye. Keda, Olga V. Khilya, Emmanuel Gras, et al.. 2-Azahetaryl-2-(oxoindolin-2-ylidene)acetonitriles as Colorimetric Probes for Zn: Synthesis and Optical Properties. ACS Omega, In press, 10.1021/acsomega.2c04747 . hal-03852505

**HAL Id: hal-03852505**

**<https://cnrs.hal.science/hal-03852505>**

Submitted on 23 Nov 2022

**HAL** is a multi-disciplinary open access archive for the deposit and dissemination of scientific research documents, whether they are published or not. The documents may come from teaching and research institutions in France or abroad, or from public or private research centers.

L'archive ouverte pluridisciplinaire **HAL**, est destinée au dépôt et à la diffusion de documents scientifiques de niveau recherche, publiés ou non, émanant des établissements d'enseignement et de recherche français ou étrangers, des laboratoires publics ou privés.

## 2-Azahetaryl-2-(oxoindolin-2-ylidenes)acetonitriles as colorimetric probes for Zn: synthesis and optical properties

Dedicated to Prof. Olga A. Zaporozhets in memoriam.

Vladyslav V. Shcherban<sup>a\*</sup>, Olena O. Kuleshova<sup>a,b</sup>, Tetiana Ye. Keda<sup>a\*</sup>, Olga V. Khilya<sup>a</sup>,  
Emmanuel Gras<sup>b,1</sup>, Yulian M. Volovenko<sup>a</sup>

<sup>a</sup> Faculty of Chemistry, Taras Shevchenko National University of Kyiv, Lva Tolstoho Street 12, Kyiv 01033, Ukraine

<sup>b</sup> Laboratoire de Chimie de Coordination, Centre National de la Recherche Scientifique, UPR8241, Université Fédérale Toulouse Midi-Pyrénées, 205, Route de Narbonne, Toulouse F-31077, France

### Abstract

A new *one-pot* approach to Zn<sup>2+</sup>-sensitive probes 2-azahetaryl-2-(oxoindolin-2-ylidenes)acetonitriles **3a-c**, **4** is described. The method includes the *in situ* formation of imidoylchloride and its further condensation with azahetarylacetonitrile **1**. The structure of the obtained compounds is studied using <sup>1</sup>H NMR, <sup>13</sup>C NMR, IR, HRMS and UV-Vis spectroscopy techniques. Two model ligands that both exhibited the highest extinction coefficient and the best solubility in Tris-buffer pH 7.2/DMSO solution, namely 5-methyl-benzothiazole derivative **3b** and benzoxazole derivative **4**, are thoroughly studied as colorimetric probes for Zn<sup>2+</sup>. The probe **3b** has the highest sensitivity to Zn<sup>2+</sup> showing a limit of ions detection (LOD) calculated by 3S-criterion of 0.43 μM and selectivity upon masking Cu<sup>2+</sup> ions with Na<sub>2</sub>S<sub>2</sub>O<sub>3</sub>. The composition of the complexes in the solution was determined by the limited logarithm method. The

---

<sup>1</sup> LHFA CNRS - UMR 5069, Université Paul Sabatier, 118, route de Narbonne, 31062 Toulouse Cedex 9

stability constant (lgK) of **3b-Zn**  $10.27 \pm 0.02$  and **4-Zn**  $12.5 \pm 0.2$ , indicates the formation of complexes of average stability.

**Keywords:** zinc probe, spectrophotometry, 2-azahetaryl-2-(oxoindolin-2-ylidenes)acetonitrile, imidoylchloride, dipyrin-like skeleton.

## 1. Introduction

Zinc is widely recognized as a “gatekeeper of the immune system”<sup>1</sup> that protects the human body against diseases, possesses antioxidant, anti-inflammatory, and antiviral activities<sup>2</sup>, including against Sars-Cov2<sup>3,4,5,6,7</sup>. To assess individual or population zinc status, various biomarkers are recommended, in particular, concentration of zinc in plasma or serum<sup>8,9,10</sup>.

From a research perspective, the recommended methods for determination of  $Zn^{2+}$  in biofluids are atomic absorption spectroscopy and inductively coupled plasma mass spectrometry<sup>11,12</sup>. Yet these methods are too expensive to be involved in routine clinical analysis. Fluorescence analyses is also the widely used technique<sup>13</sup>, however, UV-VIS spectrophotometry (SP) remains the state-of-the-art for biochemical and clinical research due to its accuracy, sensitivity, and simplicity. Despite the large number of chromophore probes for zinc<sup>14</sup> a limited number of them are used for serum and plasma SP analysis. Well-known in the range are PAR<sup>15</sup> and Zincon<sup>16</sup>, but they either do not have contrasting color transitions or sufficient selectivity or requires toxic masking agent such as cyanide ions, for example, in serum analysis with nitro-PAPS<sup>17</sup> (Figure 1).

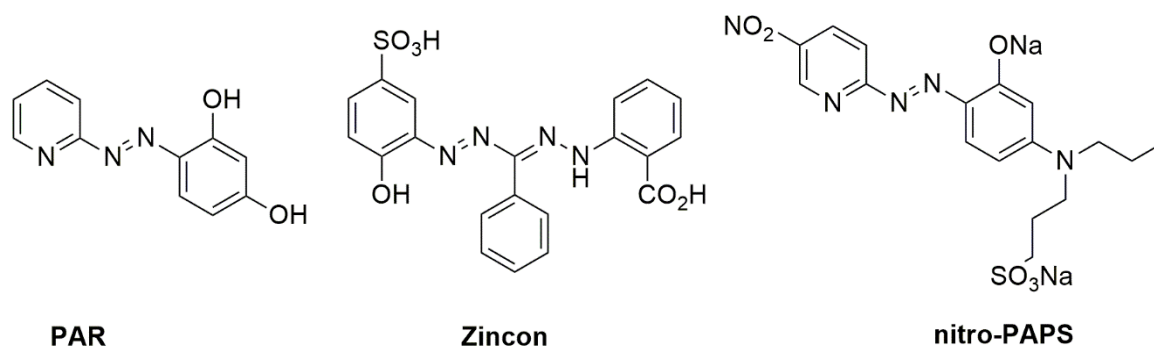
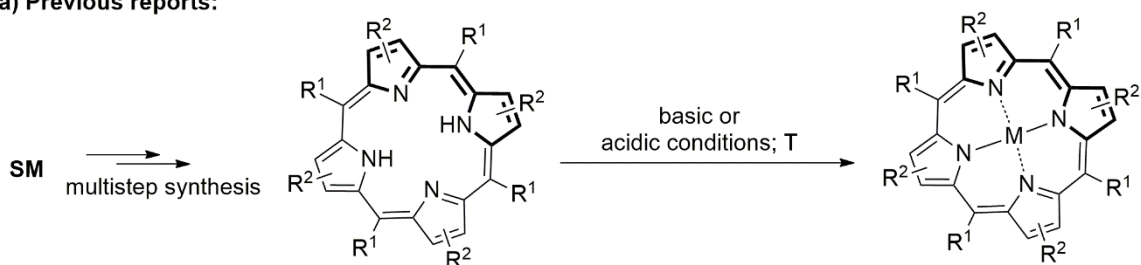


**Figure 1.** Structure of well-known chromophore probes for Zinc

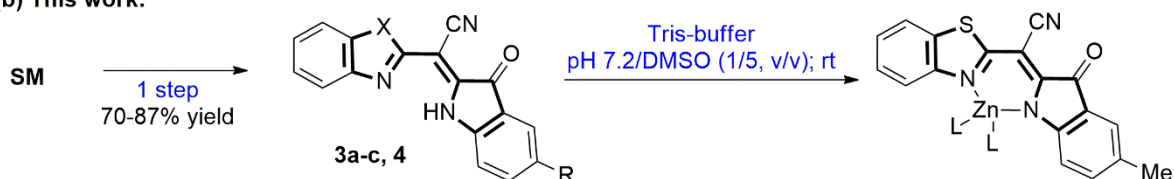
It is known that porphyrinoids because of their large conjugated system have a strong absorption peak in a visible region<sup>18</sup>. This feature correlate with their wide use as a sensitive chromogenic reagent for the detection of metal traces<sup>18,19,20,21,22</sup>. However, their coordination to metals often requires elevated temperature, auxiliaries or pH far from biologically relevant conditions<sup>18,19</sup>, probably because of the rigidity of the cavity and the required deprotonations (Figure 2a). Moreover, fast functionalization of porphyrins suffers significant synthetic limitations, thus switching their coordination and optical properties is troublesome. Multi-step synthesis of the probe is indeed usually required<sup>23</sup>.

Here we report simplified non macrocyclic analogs of porphyrins, 2-azahetaryl-2-(oxoindolin-2-ylidenes)acetonitriles **3a-c**, **4** that are easily available by *one-pot* three component reaction. Featuring the dipyrin-like skeleton they exhibit the potential for metal chelation. The representative probe **3b** can chelate Zn<sup>2+</sup> at room temperature (here after rt) in Tris-buffer, pH 7.2 /DMSO (1/5, v/v) with LOD equal to 0.43 μM and selectivity upon masking Cu<sup>2+</sup> ions (Figure 2b).

(a) Previous reports:



(b) This work:



SM - starting material

λ<sub>max2</sub> = 515-550 nm

M - metal ion

R<sup>1</sup> - any substituent at methine bridge

R<sup>2</sup> - any substituent at pyrrole subunit

**3a**: R=H; X=S; **3b**: R=Me; X=S;

**3c**: R=OMe; X=S; **4**: R=H; X=O

λ<sub>max2</sub> **3b-Zn** = 600 nm

LOD (3S) of Zn<sup>2+</sup> 0.43 μM

**Figure 2 a, b.** Porphyrinoids and their simplified analogs as metal probes.

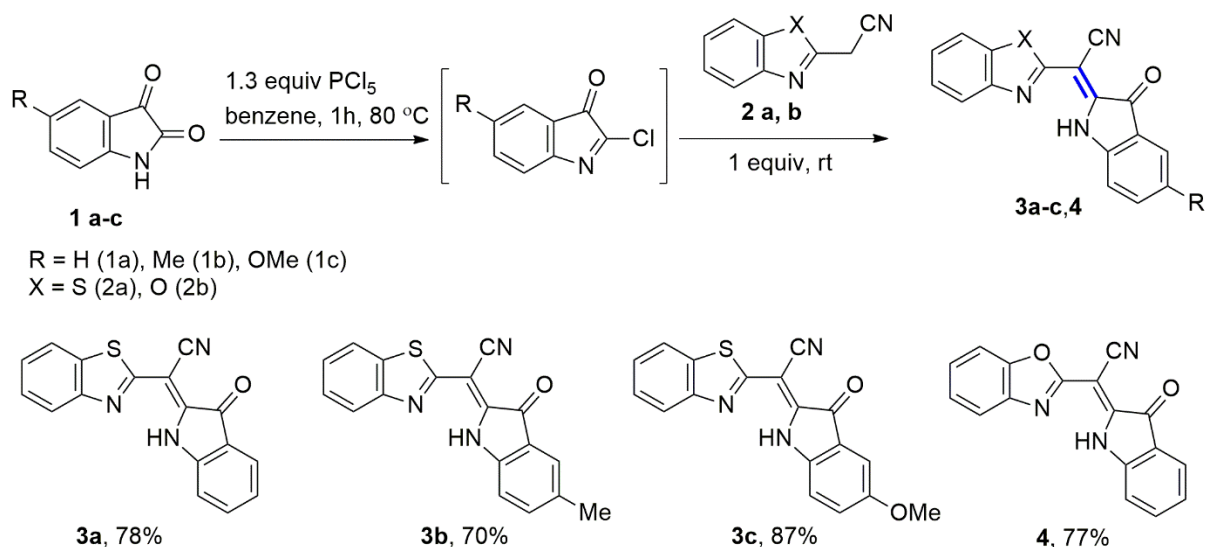
## 2. Results and discussions

### 2.1. Synthesis

In order to modulate the spectral characteristic of colorimetric probes we aimed at simplifying the structure of the well-known porphyrins. Thus, we envisaged that 2-azahetaryl-2-(oxoindolin-2-ylidenes)acetonitriles **3a-c**, **4** might be competitive with porphyrins in terms of light absorption, while they could be synthesized from commercially available isatines **2** and *N*-hetarylacetonitriles **1** synthetically easily accessible from the readily available starting materials. Moreover, kinetics of coordination of  $Zn^{2+}$  might be enhanced because of the decreased steric hindrance at the coordination site.

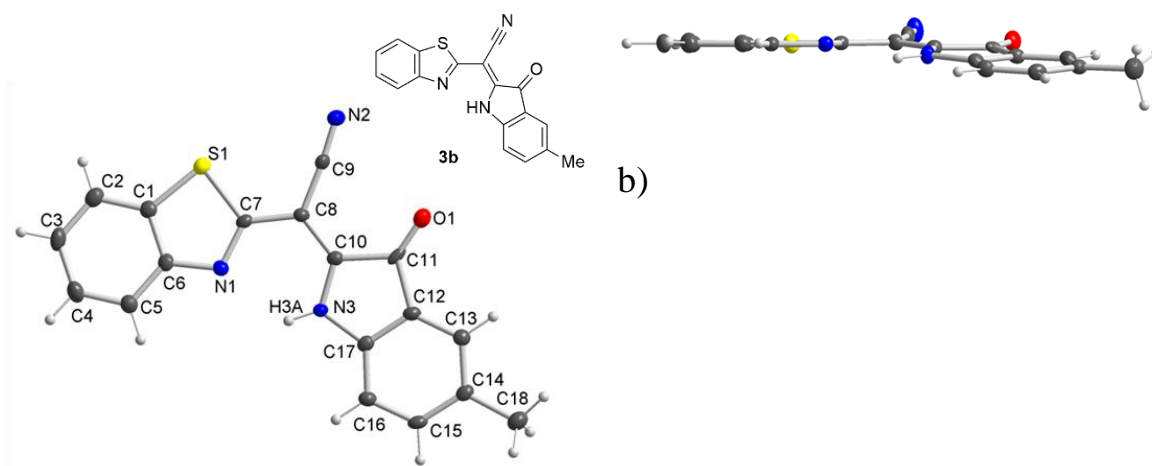
It is known that reaction of isatines with nucleophiles is directed at position 3 of isatin. In order to direct reaction at the position 2, a preactivation can be achieved by refluxing isatin and  $PCl_5$  in benzene. The resulting imidoylchloride were so far requiring isolation and dissolution in more polar solvents to perform the condensation reaction. This two-step approach decreases the yield of the product due to the poor stability of imidoylchloride promoting the formation of byproducts<sup>24,25,26</sup>.

To overcome this limitation, we have invented a *one-pot* method consisting of *in situ* formation of imidoylchloride, at the first stage and its condensation with hetarylacetonitrile **1**, at the second stage (*Scheme 1*)<sup>27</sup>. Similar three-component reactions were applied for the synthesis of 2-azahetarylenaminonitriles and reported earlier by our group<sup>28</sup>.



**Scheme 1.** Synthesis of dyes **3a-c, 4**

The limiting reaction step is the generation of imidoylchloride and the reaction is over within an hour. The yield of the products varies from 70% to 87% and their purification is performed by simple filtration through a plug of silica gel using dichloromethane as an eluent. In  $^1\text{H}$  NMR spectra of **3a-c, 4** the characteristic broaden peak of the proton of amino group shifted toward the deshielded side ( $\delta = 11.4\text{--}12.0$  ppm). Most likely the reason for this occurrence is the intramolecular hydrogen bond that forms between nitrogen of azaheterocycle and hydrogen of indolinone backbone. Single crystals of **3b** were grown by gas diffusion method from  $\text{CHCl}_3/\text{hexane}$ , XRD allowed the full assessment of the molecular structure (Figure 3).



a)

**Figure 3.** Molecular structure of **3b** according to X-Ray diffraction with the atom numbering used in the crystallographic analysis. a) a planar projection; b) an orthogonal projection.

According to XRD of **3b** estimated length of hydrogen bond N3H3A $\cdots$ N1 is 2.15 Å, the angle N3–H3A $\cdots$ N1 is equal to 123.3°. The dihedral angle between heterocycles planes is equal to 8.8°, which indicates an effective delocalization of charge in the molecule, promoting the shift of the NH in  $^1\text{H}$  NMR to the deshielded side.

A complete assignment of the peaks at  $^1\text{H}$  and  $^{13}\text{C}$  NMR was accomplished using 2D NMR techniques (COSY, HMBC and HMQC).

A library of ligands has been synthesized to modulate the donating properties of the R substituent as well as the nature and electronic properties of the attached heterocycle. Thus, a library of compounds has been accessed based on either benzothiazole (**3**) or benzoxazole (**4**) from a reaction with unsubstituted isatin (**a**), isatin featuring a  $\sigma$ -donor such as a methyl group (**b**), or a  $\pi$ -donor such as a methoxy group (**c**).

## 2.2. Photophysical properties

2-azahetaryl-2-(5-R-3-oxoindoline-2-ylidene)acetonitriles are characterized by the rich color ranging from red to purple. The non-substituted isatin compounds **3a** and **4** in DMSO featured absorption spectra with a long wave band

at 425-600 nm and the maximum centered around 520 and 515 nm respectively (Figure 4, Table 1). Methyl- and methoxy-substitute compounds **3b** and **3c** in DMSO featured absorption spectra with maximum centered around 530 and 550 nm respectively and the shoulders at 650-750 nm. The increased bathochromic shift of substituted dyes comparing to non-substituted may be rationalized by the presence of electron density donors at oxoindolinone core consequently the shrinking of HOMO–LUMO gap.

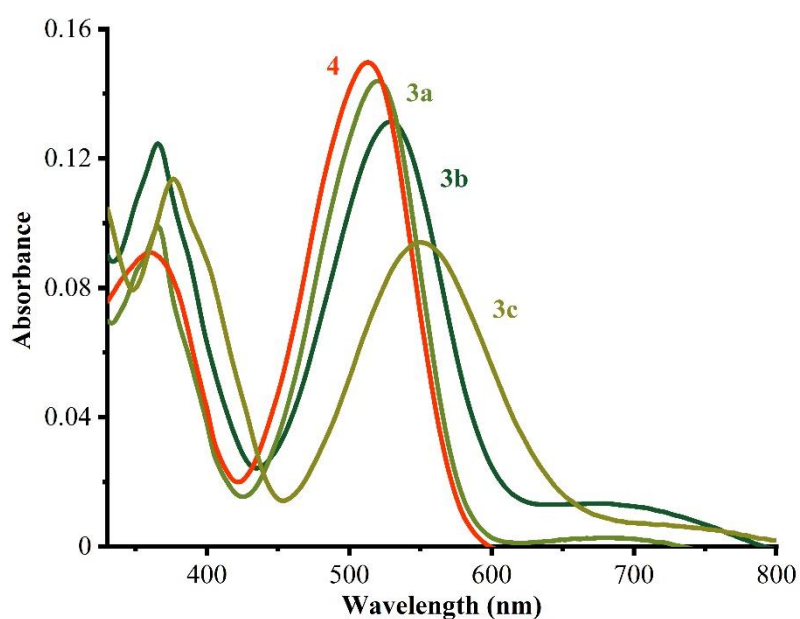


**Figure 4.** Absorption spectra of dyes **3a-c** and **4** in DMSO solution.  $C = 10 \mu\text{mol}\cdot\text{L}^{-1}$ ,  $l=1.00 \text{ cm}$

**Table 1.** Spectrophotometric characteristics of dyes **3a-c** and **4** in DMSO solution.

Dye	$\lambda_{\text{max1}}$ , nm	$\epsilon_{\lambda_{\text{max1}}}$ , $\text{mol}^{-1}\text{Lcm}^{-1}$ , $10^4$	$\lambda_{\text{max2}}$ , nm	$\epsilon_{\lambda_{\text{max2}}}$ , $\text{mol}^{-1}\text{Lcm}^{-1}$ , $10^4$
<b>3a</b>	363	$1.10\pm 0.11$	520	$1.48\pm 0.05$
<b>3b</b>	367	$1.37\pm 0.07$	530	$1.38\pm 0.05$
<b>3c</b>	376	$1.26\pm 0.05$	550	$1.03\pm 0.05$
<b>4</b>	357	$1.09\pm 0.14$	515	$1.66\pm 0.10$

### 2.3. Photostability test

To assess the stability of dyes in DMSO solutions, UV-Vis absorption spectra were recorded after 24, 72, 96 h and 6 months of exposure to indirect

light. The absorbance of the solutions was unchanged, which indicates a high photostability of the dye solutions (See SI Figure S14).

#### 2.4. UV-Vis spectra in H<sub>2</sub>O/DMSO solutions

Water solubility of 2-azahetaryl-2-(5-R-3-oxoindolin-2-ylidene)acetonitriles affects seriously their spectroscopic and chemical properties. The influence of water on the absorption spectra of the dyes **3a**, **3b** and **4** in DMSO and the values of their molar absorption coefficient ( $\epsilon$ ) were studied (See SI Section 3). The molar absorption coefficient change was calculated as  $\Delta\epsilon_{\max, \%} = (\epsilon_{\max \text{ DMSO}} - \epsilon_{\max \text{ H}_2\text{O/DMSO}})100/\epsilon_{\max \text{ DMSO}}$ , where  $\epsilon_{\max \text{ DMSO}}$  and  $\epsilon_{\max \text{ H}_2\text{O/DMSO}}$  – molar absorption coefficient of dyes at  $\lambda_{\max}$  in DMSO and H<sub>2</sub>O/DMSO mixture with different solvents ratio (v/v), respectively. Apparently dyes **3b** and **4** were found to be the most hydrophilic compounds at H<sub>2</sub>O/DMSO (1/(1.5 to 5), v/v) mixtures. The decreasing of molar absorption coefficient was not more than 10% ( $\Delta\epsilon_{\max} \leq 10\%$ ), while the decreasing of the absorbance value up to 50% were observed for dye **3a** (See SI Table S2). Based on this observation the dyes **3b** and **4** were chosen for the next studies.

The deprotonation of molecules **3b** and **4** at NH site upon titration with alkaline solution is demonstrated at Figures 5-6. The isosbestic points located at 584 nm for **3b** and 562 nm for **4** indicate the coexistence of two forms (neutral and anionic) of dyes in alkaline solutions. The bathochromic shifts ( $\Delta\lambda$ ) of the absorption bands of neutral forms ( $\lambda_{\max}=530$  nm (**3b**) and  $\lambda_{\max}=515$  nm (**4**)) to anionic forms are equal to 150 nm for **3b** and 130 nm for **4** which corresponds to drastic color change from purple to turquoise visible by a naked eye. These transitions were shown to be reversible. The bathochromic shift occurring under basic conditions may be rationalized by the formation of an anion which characterized by the facilitated oscillation of the  $\pi$ -electrons compared to the neutral form. Therefore, less energy is required to excite the electrons, which causes a long wavelength  $\pi \rightarrow \pi^*$  electronic transition (See SI Scheme S1).

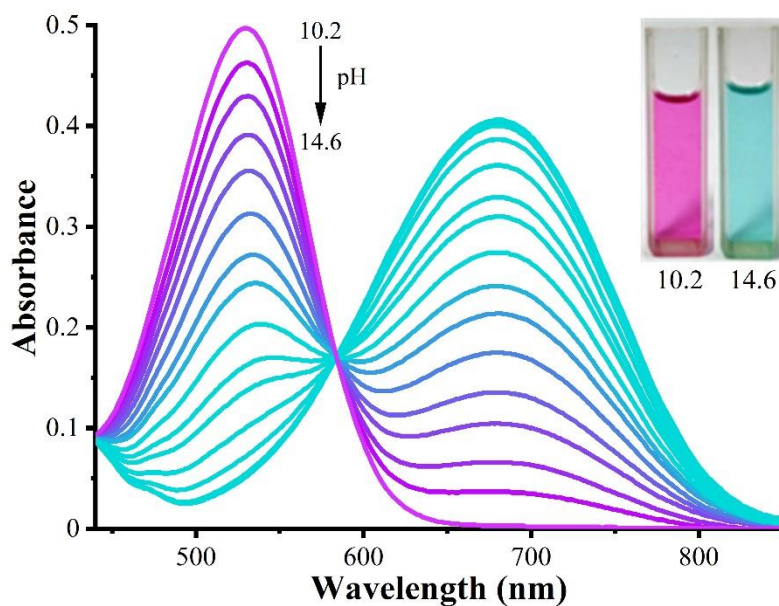


**Figure 5.** Absorption spectra of  $40 \mu\text{mol}\cdot\text{L}^{-1}$  **3b** in  $\text{H}_2\text{O}/\text{DMSO}$  (1/5, v/v) upon addition of different amount of NaOH. Photographs of neutral (left) and anionic (right) form of dye in solution with appropriate pH are shown in the inset.  $\ell = 1.00 \text{ cm}$ .

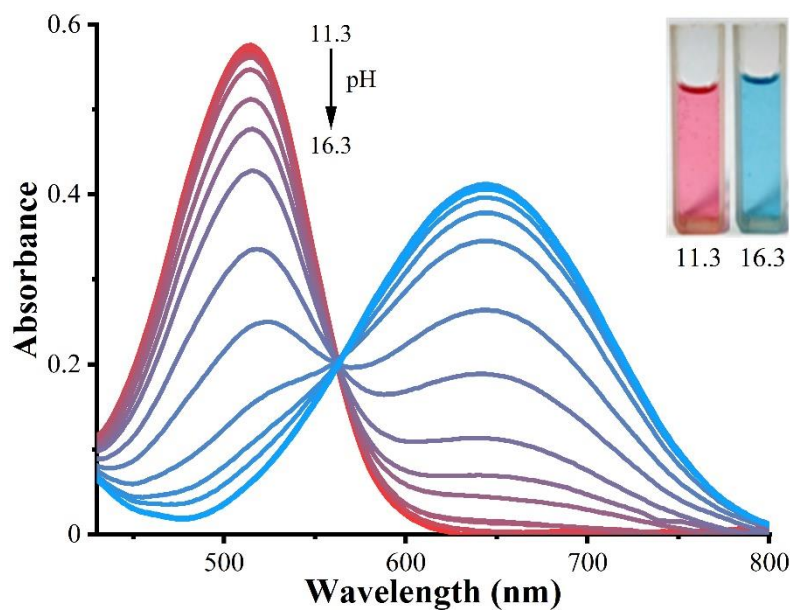


**Figure 6.** Absorption spectra of  $40 \mu\text{mol}\cdot\text{L}^{-1}$  **4** in  $\text{H}_2\text{O}/\text{DMSO}$  (1/3, v/v) upon addition of different amount of NaOH. Photographs of neutral (left) and anionic (right) form of dye in solution with appropriate pH are shown in the inset.  $\ell = 1.00 \text{ cm}$ .

The apparent ionization constants (pKa) values of molecules **3b** and **4** in H<sub>2</sub>O/DMSO mixture have been obtained with spectrophotometric titrations according to the Equation 1, section 4.3. (Table 2, See SI Tables S4, S5).

**Table 2.** Apparent ionization constants of the dyes **3b** and **4** in H<sub>2</sub>O/DMSO solutions.

Dye	H <sub>2</sub> O/DMSO (v/v)	pKa
<b>3b</b>	1/5	13.7 ± 0.1
<b>4</b>	1/3	15.2 ± 0.2

### 2.5. Interaction with Zn<sup>2+</sup>

It was envisioned that dyes **3b** and **4** can chelate Zn<sup>2+</sup> due to the presence of dipyrin-like skeleton.<sup>29</sup> Indeed, upon addition of Zn<sup>2+</sup> to the solution of **3b** and **4** the hyperchromic effect occurs at 600 and 565 nm respectively. Meanwhile, the color changes from purple (**3b**) and red (**4**) to blue which corresponds to the bathochromic shift of  $\lambda_{\max}$  at UV-vis spectra (Figure 7 and 8). Such changes may probably indicate the formation of the complexes. The most convenient environment for the interaction of the ligand and Zn<sup>2+</sup> was chosen based on two factors: the largest achievable light absorption of the complex at the appropriate wavelength (to ensure the highest detection sensitivity) and the lowest possible DMSO content. Having this in mind and considering the studies data presented in SI Figures S17 (b), S18, Table S3 the ratio of Tris-buffer (pH 7.2) and DMSO 1/5 (**3b**) and 1/3 (**4**) was the best.

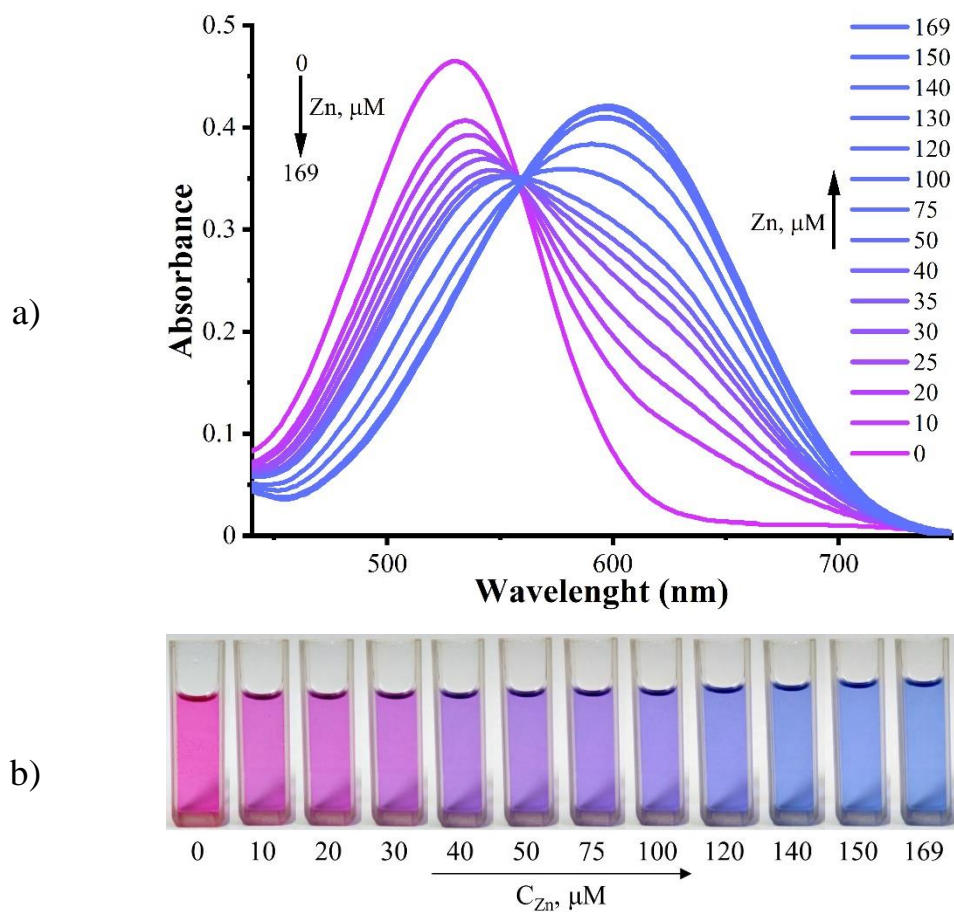


**Figure 7.** Absorption spectra of dye **3b** without and in the presence of different amount of  $\text{Zn}^{2+}$ ,  $C_{3b} = 38 \mu\text{mol}\cdot\text{L}^{-1}$ , Tris-buffer (pH 7.2)/DMSO (1/5, v/v) (a), photographs of dye **3b** in the presence of different amount of  $\text{Zn}^{2+}$  (b); Concentration of  $\text{Zn}^{2+}$  is shown in the insets.

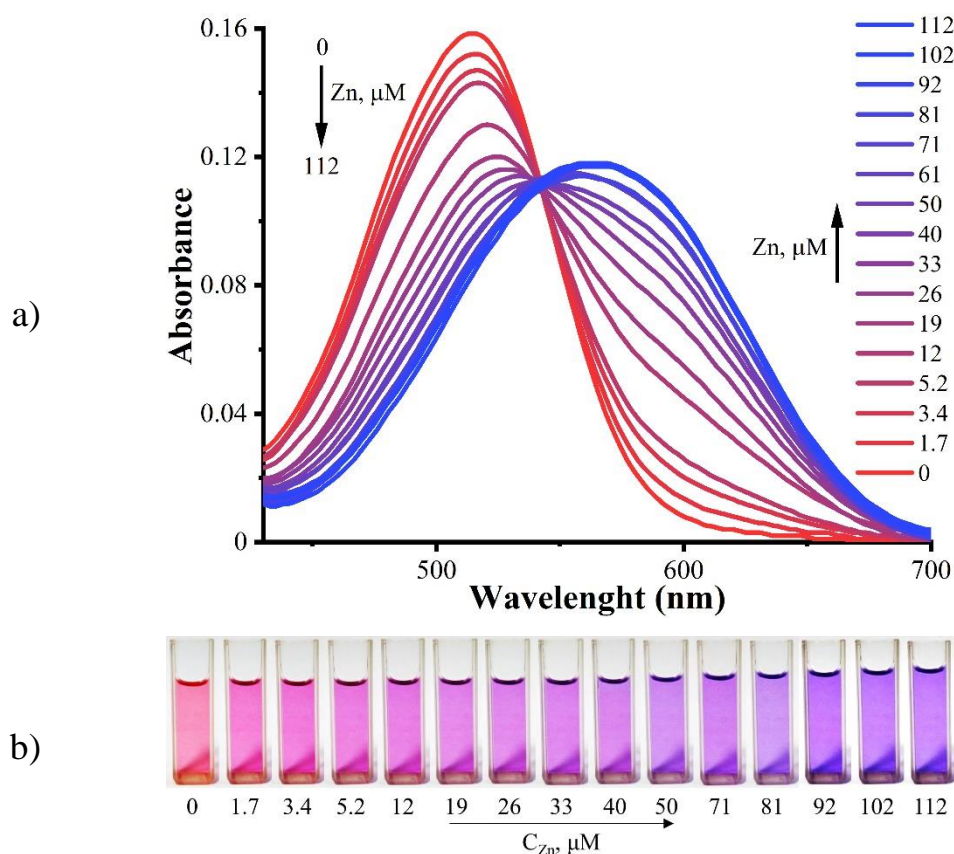


**Figure 8.** Absorption spectra of dye **4** without and in the presence of different amount of Zn<sup>2+</sup>,  $C_4 = 9.9 \mu\text{mol}\cdot\text{L}^{-1}$ , Tris-buffer (pH 7.2)/DMSO (1/3, v/v) (a); photographs of dye **4** in the presence of different amount of Zn<sup>2+</sup> (b); Concentration of Zn<sup>2+</sup> is shown in the insets.

The classical, the Bent and French method<sup>30</sup> were applied to spectral data processing. Considering the shape of the saturation curves in Figure 9-10, it can be assumed that a medium stability complex is formed in the solutions. The molar composition of complexes ( $\text{Zn}_m\text{R}_n$ ) was established as described in section 4.4. The calculations gave the values of  $n/m$  are equal to 1 for both complexes of probes **3b** and **4** with Zn<sup>2+</sup>, which confirmed the formation of ZnR complexes in solutions. Under these conditions, the neutral forms of probes appeared to be predominant in the solutions (See SI Figure S19).

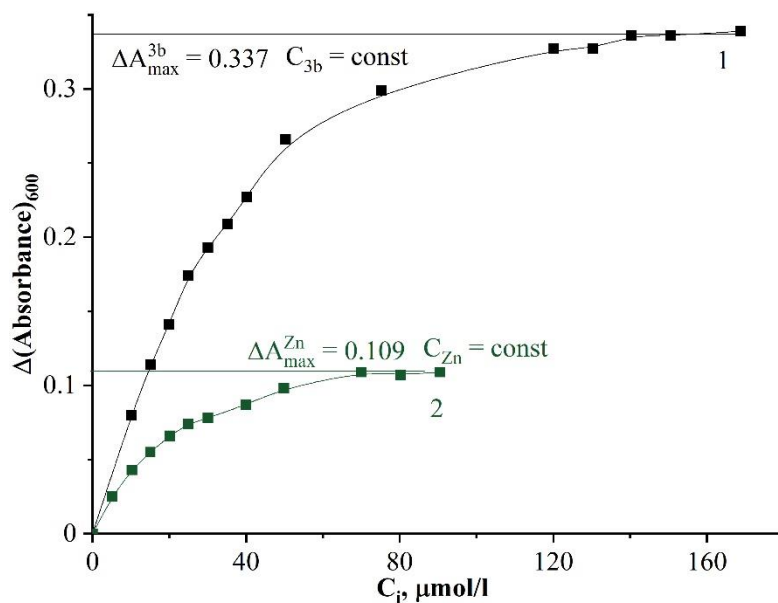


**Figure 9.** Saturation curves of the complex formation between  $\text{Zn}^{2+}$  and probe **3b** in Tris-buffer (pH 7.2)/DMSO (1/5, v/v).  $C(\mathbf{3b}) = 38 \mu\text{mol}\cdot\text{L}^{-1}$  (1);  $C(\text{Zn}^{2+}) = 10 \mu\text{mol}\cdot\text{L}^{-1}$  (2).

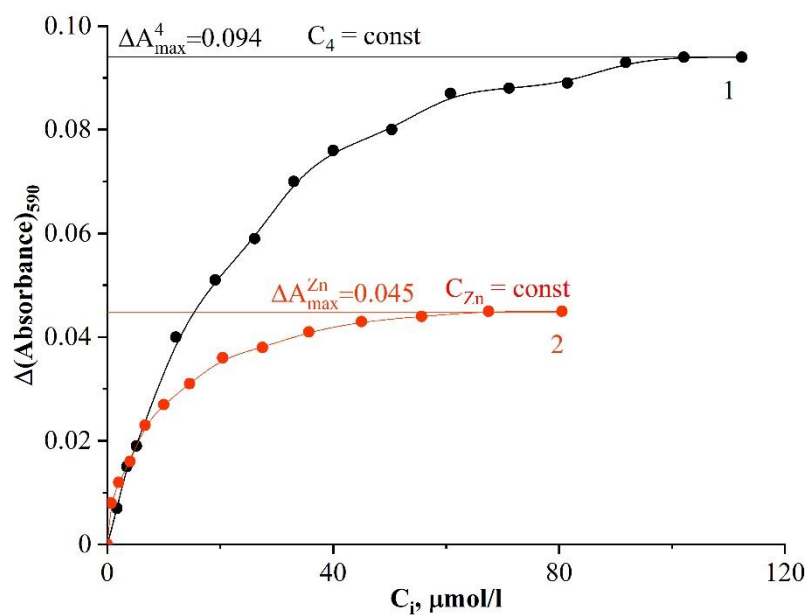


**Figure 10.** Saturation curves of the complex formation between  $\text{Zn}^{2+}$  and probe **4** in Tris-buffer (pH 7.2)/DMSO (1/3, v/v).  $C(\mathbf{4}) = 10 \mu\text{mol}\cdot\text{L}^{-1}$  (1);  $C(\text{Zn}^{2+}) = 5 \mu\text{mol}\cdot\text{L}^{-1}$  (2).

The stability constants of the complexes **3b-Zn** and **4-Zn** have been calculated by processing the data from the saturation curves (Figure 9, 10) using Equation 2 (See SI Section 5). The values of the affinity constants were found to be equal  $\lg K^f = 10.27 \pm 0.02$  and  $\lg K^f = 12.5 \pm 0.2$  for probes **3b** and **4**, respectively.

### 2.6. Spectrophotometric determination of $Zn^{2+}$

Hence, the absorbance of probes **3b** and **4** at maximum of the complexes after treatment with the  $Zn^{2+}$  solutions was also found depend on their concentration. The dependence of the absorption maxima and absorbance at the wavelength ranges with minimum spectra overlap is consistent with the Beer-Lambert law in the wide  $Zn^{2+}$  concentration ranges (Table 3).

**Table 3.** Performance characteristics of  $Zn^{2+}$  spectrophotometric determination. ( $\Delta A_\lambda = A_{\lambda_i} - A_{\lambda_0}$ ,  $n=6$ ,  $P=0.95$ )

Dye	Regression equation	RSD <sup>2</sup>	Linear range, $\mu\text{mol}\cdot\text{L}^{-1}$	LOD (3S), $\mu\text{mol}\cdot\text{L}^{-1}$
<b>3b</b>	$\Delta A_{640}=(0.003\pm 0.001) + (0.0103\pm 0.0001)\cdot C_{Zn}, \mu\text{mol}\cdot\text{L}^{-1}$	0.999	1.0 - 20.0	0.43
	$\Delta A_{600}=(0.005\pm 0.002) + (0.0111\pm 0.0002)\cdot C_{Zn}, \mu\text{mol}\cdot\text{L}^{-1}$	0.998		0.54
<b>4</b>	$\Delta A_{610}=(0.0013\pm 0.0009) + (0.0028\pm 0.0002)\cdot C_{Zn}, \mu\text{mol}\cdot\text{L}^{-1}$	0.992	1.7 - 12.1	0.96
	$\Delta A_{590}=(0.002\pm 0.001) + (0.0032\pm 0.0002)\cdot C_{Zn}, \mu\text{mol}\cdot\text{L}^{-1}$	0.990		0.94

The dye **3b** has better characteristic due to the wider linearity of  $Zn^{2+}$  concentration range and higher sensitivity. The selectivity of dyes **3b** towards  $Zn^{2+}$  was appraised by titration of the probe with various metal ions at the optimal conditions of zinc complexes formation (See SI Section 6). It was shown that

heavy metal ions such as  $\text{Fe}^{3+}$ ,  $\text{Fe}^{2+}$ ,  $\text{Ni}^{2+}$  and  $\text{Cd}^{2+}$  did not affect the absorption of dye **3b** (See SI Figure S22). As expected only  $\text{Co}^{2+}$  and  $\text{Cu}^{2+}$  cause significant change in colors of solutions. But the change of the color in the presence of  $\text{Co}^{2+}$  is very slow process and the absorption spectra change could be observed after 30 min of solutions treatment with  $\text{Co}^{2+}$  (See SI Figure S23). Due to this fact the presence of equal amount of  $\text{Co}^{2+}$  does not interfere with  $\text{Zn}^{2+}$  determination during 20 min after probe treatment. It was found that  $\text{Cu}^{2+}$  ions could be masked using  $1.0 \text{ mmol}\cdot\text{L}^{-1}$   $\text{Na}_2\text{S}_2\text{O}_3$  solution (See SI Figure S24).

To prove the reliability of the technique the probe **3b** was applied to detecting of  $\text{Zn}^{2+}$  in serum model solution (stripped of protein) (See SI Section 7). The model solution of 2 times diluted pre-treated blood serum were prepared as recommended in<sup>31</sup> using standard solutions of  $\text{Zn}^{2+}$ ,  $\text{Cu}^{2+}$ ,  $\text{Fe}^{2+}$ ,  $\text{Na}^+$ ,  $\text{K}^+$ ,  $\text{Ca}^{2+}$ ,  $\text{Mg}^{2+}$  and Tris-buffer (pH=7.2). The resulting samples were analyzed spectrophotometrically. For this purpose, 2.5 mL of  $40 \text{ }\mu\text{mol}\cdot\text{L}^{-1}$  of probe **3b** solution in DMSO was mixed with 0.5 mL of model solution in Tris-buffer (pH=7.2) in the presence of  $\text{Na}_2\text{S}_2\text{O}_3$  and the absorbance of solutions were measured. The recovery value does not exceed of 105% for 5.0 and  $10.0 \text{ }\mu\text{mol}\cdot\text{L}^{-1}$  of spiked  $\text{Zn}^{2+}$  in sample was observed. The data obtained suggest that proposed technique could be used for  $\text{Zn}^{2+}$  determining in real samples. Full method validation using real samples will be the aim of our further work.

A comparison of probe **3b** with other reported colorimetric probes for  $\text{Zn}^{2+}$  in complex matrices has shown that the closest analogue of probe **3b** in terms of sensitivity, metal ions selectivity and contrasting colour change accompanying the complexation is Zincon (See SI Table S9). Moreover, probe **3b** demonstrates much better stability in solutions than Zincon<sup>16</sup>. High DMSO content in a sample solution does not interfere with the determination of Zn total amount in the pretreated bio-samples using probe **3b**.

### 3. Conclusion

In summary, we have developed a *one-pot* approach for the synthesis of 2-azahetaryl-2-(oxoindolin-2-ylidenes)acetonitriles via *in situ* formation of imidoylchloride and we have found that these dyes are sensitive probes for Zn<sup>2+</sup> ions when Cu<sup>2+</sup> ions are masked with Na<sub>2</sub>S<sub>2</sub>O<sub>3</sub>. The best analytical response is demonstrated by benzothiazole derivative **3b** with LOD 0.43 μM in Tris-buffer pH 7.2/DMSO solution. Contrasting color change accompanying the complex formation, as well as stability of the dye and its complex with zinc, make possible the highly sensitive and selective determination of Zn<sup>2+</sup> ions using UV-Vis spectrophotometry. Therefore, probe **3b** is promising for detecting and monitoring Zn<sup>2+</sup> ions in biological fluids, such as serum.

### 4. Experimental section<sup>32</sup>

#### 4.1. Materials and methods

All chemicals and solvents were analytical grade and used without further purification. Isatin **2a**, 5-methylisatin **2b**, 5-methoxyisatin **2c** were provided by Enamine Ltd. 2-(Benzo[*d*]thiazol-2-yl)acetonitrile **1a** was synthesized by a known method<sup>33</sup>. 2-(Benzo[*d*]thiazol-2-yl)acetonitrile **1b** was synthesized as described below in the synthesis section.

Preparative chromatography was performed manually with silica gel (63–200 μm).

<sup>1</sup>H NMR and <sup>13</sup>C{<sup>1</sup>H} NMR spectra were recorded on a Bruker Avance 300 (300 and 75 MHz respectively) or a Bruker Avance III 400 (400 and 101 MHz respectively) spectrometer and were referenced to the residual proton resonances of the DMSO-*d*<sub>6</sub>: 2.50 for <sup>1</sup>H and 40.0 ppm for <sup>13</sup>C. The degree of carbon atom substitution was determined by NMR spectra acquired according to the DEPT-135 or JMOD methods. Two-dimensional (2D) (COSY, HMQC, HMBC) spectra were recorded on a Bruker Avance III 400 spectrometer and Bruker Avance 500. All spectra were recorded at ambient temperature (298 K). Coupling constants

(*J*), are reported in Hz, chemical shift ( $\delta$ ) in ppm. The multiplicity of signals is indicated using the following abbreviations: s = singlet, bs = broad singlet, d = doublet, t = triplet, q = quartet, quint = quintet, dd = doublet of doublets, ddd = doublet of doublets of doublets, dt = doublet of triplets, m = multiplet and br = broad.

IR spectra recorded on FT-IR spectrometer Perkin Elmer in KBr plates.

High resolution mass spectra (HRMS) were recorded on GCT Premier spectrometer upon electron spray ionization (ESI) or chemical ionization (DCI, CH<sub>4</sub>).

Melting points were determined on a Boetius micro hot stage apparatus with VEB Analytik 1399RNMK 05 observation lens.

X-Ray crystallography was performed on single crystal diffractometer Agilent Gemini. Gas diffusion method were implemented for single crystals growing.

Absorption spectra were recorded on a SHIMADZU UV-2401 PC spectrophotometer. pH measurements were performed with a STARTER 3100 Bench pH Meter (OHAUS).

#### *4.2. Synthesis*

##### **2-(Benzo[d]oxazol-2-yl)acetonitrile**

A solution of 2-aminophenol (4.36 g, 40 mmol) and 2-cyanoacetimidate hydrochloride<sup>34</sup> (6.36 g, 44 mmol) in anhydrous CH<sub>2</sub>Cl<sub>2</sub> (110 ml) was heated to reflux over a 10 h period (TLC elution system: CHCl<sub>3</sub>:CH<sub>3</sub>OH (9:1)). The reaction mixture was then cooled down, diluted with CH<sub>2</sub>Cl<sub>2</sub> (110 ml) and washed with 10% NaOH solution until the discoloration of water layer. The organic layer was dried over MgSO<sub>4</sub> and concentrated under reduced pressure to yielded desired compound. 4.43 g of the product (28 mmol, 70 % yield) was obtained as a beige solid. **<sup>1</sup>H NMR (400 MHz, Chloroform-*d*)**  $\delta$  4.13 (s, 2H), 7.37 – 7.45 (m, 2H), 7.55 – 7.60 (m, 1H), 7.74 – 7.79 (m, 1H). The compound was used in the next step without further purification.

**General procedure for the synthesis of 2-hetaryl-2-(5-R-3-oxoindolin-2-ylidene)acetonitriles 3a-c, 4.** To the strongly stirred suspension of 5-R-isatine (1 mmol) in hot benzene (10 ml – 15 ml) the phosphorus pentachloride (1.3 mmol) was added. The resulting mixture was refluxed over 1 hour. At this point, solution of hetarylacetonitrile (1 mmol) in benzene was added drop wise and characteristic change of the color occurred. The mixture was allowed to cool to room temperature upon stirring. The precipitate was then filtrated and washed with minimum amount of ethanol, water and again with ethanol. Dry precipitate was purified by filtration through the plug of silica gel (eluent: CH<sub>2</sub>Cl<sub>2</sub>)

**(Z)-2-(benzo[d]thiazol-2-yl)-2-(3-oxoindolin-2-ylidene)acetonitrile 3a.** The product (236 mg, 0.78 mmol, 78% yield) was obtained as a dark red powder (mp > 300 °C) from 147 mg (1 mmol) of isatin **1a** and 174 mg (1 mmol) of 2-(benzo[d]thiazol-2-yl)acetonitrile **2a**. **IR (KBr):** 3408, 2205, 1712, 1589. **<sup>1</sup>H NMR (400 MHz, DMSO-*d*<sub>6</sub>)** δ 7.16 (td, *J* = 7.5, 0.8 Hz, 1H, 5-H<sub>IS</sub>), 7.50 – 7.56 (m, 2H, 5-H<sub>BT</sub>, 7-H<sub>IS</sub>), 7.66 (ddd, *J* = 8.2, 7.8, 1.1 Hz, 1H, 6-H<sub>BT</sub>), 7.66 – 7.71 (m, 1H, 6-H<sub>IS</sub>), 7.73 (d, *J* = 7.6 Hz, 1H, 4-H<sub>IS</sub>), 8.20 (d, *J* = 8.1, 1.0, 0.6 Hz, 1H, 7-H), 8.21 (d, *J* = 8.0, 1.3, 0.6 Hz, 1H, 4-H), 11.55 (s, 1H, NH). **<sup>13</sup>C{<sup>1</sup>H} NMR (101 MHz, DMSO-*d*<sub>6</sub>)** δ 80.2 (C), 114.5 (CH), 116.9 (C), 119.9 (C), 123.0 (CH), 123.2 (CH), 123.6 (CH), 125.7 (CH), 126.4 (CH), 127.6 (CH), 134.3 (C), 138.2 (CH), 143.7 (C), 151.9 (C), 154.0 (C), 163.4 (C), 185.1 (C). **HRMS (ESI)** calcd for C<sub>17</sub>H<sub>10</sub>N<sub>3</sub>OS (M + H<sup>+</sup>) 304.0545, found 304.0545.

**(Z)-2-(benzo[d]thiazol-2-yl)-2-(5-methyl-3-oxoindolin-2-ylidene)acetonitrile 3b.** The product (222 mg, 0.7 mmol, 70% yield) was obtained as a dark red powder (mp 300–301 °C) from 161 mg (1 mmol) of 5-methylisatin **1b** and 174 mg (1 mmol) of 2-(benzo[d]thiazol-2-yl)acetonitrile **2a**. **IR (KBr):** 3433, 2204, 1718, 1596. **<sup>1</sup>H NMR (400 MHz, DMSO-*d*<sub>6</sub>)** δ 2.33 (s, 3H), 7.40 (d, *J* = 8.2 Hz, 1H), 7.47 – 7.53 (m, 2H), 7.54 (s, 1H), 7.65 (ddd, *J* = 8.2, 7.6, 1.1 Hz, 1H), 8.18 (d, *J* = 7.8 Hz, 1H), 8.20 (d, *J* = 7.7 Hz, 1H), 11.48 (s, 1H). **<sup>13</sup>C{<sup>1</sup>H} NMR (101 MHz, DMSO-*d*<sub>6</sub>)** δ 20.6 (CH<sub>3</sub>), 79.7 (C), 114.3 (CH), 116.9 (C),

120.0 (C), 122.9 (CH), 123.1 (CH), 125.6 (CH), 126.3 (CH), 127.6 (CH), 133.1 (C), 134.3(C), 138.8 (CH), 143.9 (C), 150.0 (C), 154.0 (C), 163.5 (C), 185.1 (C). **HRMS** (ESI) calcd for C<sub>18</sub>H<sub>12</sub>N<sub>3</sub>OS (M + H<sup>+</sup>) 318.0701, found 318.0704. CCDC deposition number: 2176039

**(Z)-2-(benzo[d]thiazol-2-yl)-2-(5-methoxy-3-oxoindolin-2-ylidene)acetonitrile 3c.** The product (290 mg, 0.87 mmol, 87% yield) was obtained as a dark violet powder (mp 297–298 °C) from 177 mg (1 mmol) of isatin **1c** and 174 mg (1 mmol) of 2-(benzo[d]thiazol-2-yl)acetonitrile **2a**. **IR (KBr):** 3428, 2201, 1702, 1591, 1213. **<sup>1</sup>H NMR (400 MHz, DMSO-*d*<sub>6</sub>)** δ 3.81 (s, 1H), 7.25 (d, *J* = 2.2 Hz, 1H), 7.28 (dd, *J* = 8.6, 2.5 Hz, 1H), 7.44 (d, *J* = 8.6 Hz, 1H), 7.52 (t, *J* = 7.5 Hz, 1H), 7.65 (t, *J* = 7.7 Hz, 1H), 8.20 (d, *J* = 8.0 Hz, 1H), 8.18 (d, *J* = 8.2 Hz, 1H), 11.42 (s, 1H). **<sup>13</sup>C{<sup>1</sup>H} NMR (101 MHz, DMSO-*d*<sub>6</sub>)** δ 56.3 (CH<sub>3</sub>), 79.6 (C), 108.9 (CH), 115.5 (C), 117.0 (C), 120.4 (C), 122.9 (CH), 123.1 (CH), 125.2 (CH), 126.2 (CH), 127.6 (CH), 134.2 (CH), 144.1 (C), 146.2 (C), 154.1 (C), 156.2 (C), 163.5 (C), 185.1 (C). **HRMS** (ESI) calcd for C<sub>18</sub>H<sub>12</sub>N<sub>3</sub>O<sub>2</sub>S (M + H<sup>+</sup>) 334.0650, found 334.0647.

**(Z)-2-(benzo[d]oxazol-2-yl)-2-(3-oxoindolin-2-ylidene)acetonitrile 4.** The product (221 mg, 0.77 mmol, 77% yield) was obtained as a dark red powder (mp > 300 °C) from 147 mg (1 mmol) of isatin **1a** and 158 mg (1 mmol) of 2-(benzo[d]oxazol-2-yl)acetonitrile **2b**. **IR (KBr):** 3435, 2214, 1719, 1596. **<sup>1</sup>H NMR (400 MHz, DMSO-*d*<sub>6</sub>)** δ 7.16 (td, *J* = 7.4, 0.8 Hz, 1H, 5-H<sub>Is</sub>), 7.47 – 7.51 (m, 2H, 5,6-H<sub>Bzo</sub>), 7.52 – 7.55 (m, 1H, 7-H<sub>Is</sub>), 7.67 (td, *J* = 7.8, 1.3 Hz, 1H, 6-H<sub>Is</sub>), 7.72 (d, *J* = 7.5 Hz, 1H, 4-H<sub>Is</sub>), 7.83 – 7.90 (m, 2H, 4,7-H<sub>Bzo</sub>), δ 11.37 (s, 1H, NH). **<sup>13</sup>C{<sup>1</sup>H} NMR (101 MHz, DMSO-*d*<sub>6</sub>)** δ 74.0 (C), 111.6 (CH), 114.5 (C), 114.6 (CH), 119.97 (C), 120.01 (CH), 123.8 (CH), 125.7 (CH), 126.0 (CH), 126.6 (CH), 138.3 (CH), 141.7 (C), 145.9 (C), 149.9 (C), 151.7 (C), 159.5 (C), 184.6 (C). **HRMS** (ESI) calcd for C<sub>17</sub>H<sub>10</sub>N<sub>3</sub>O<sub>2</sub> (M + H<sup>+</sup>) 288.0773, found 288.0773. CCDC deposition number: 2176040

#### 4.3. *pKa determination*

The apparent ionization constant ( $pK_a$ ) values of the compounds **3b** and **4** were determined spectrophotometrically.<sup>35</sup> Titration 3.00 ml of 40  $\mu\text{mol}\cdot\text{L}^{-1}$  of each compound was performed in a  $\text{H}_2\text{O}/\text{DMSO}$  by adding small portions 0.010 - 0.10 M HCl or NaOH solutions and recording the absorption spectrum after each addition. Solution volume has not changed by more than 10%.

The calculation of apparent ionization constants was carried out using the absorption data according Henderson-Hasselbalch equation:

$$K_a^f = \frac{A_i - A_{HR}}{A_R - A_i} \cdot 10^{-pH}, \quad (1)$$

where  $A_{HR}$  is the absorbance of the solution at the absorption maximum of the molecular form of the dye,  $A_R$  is the absorbance of the solution at the absorption maximum of the ionic form of the dye,  $A_i$  is the absorbance of the solution at the absorption maximum of the mixture of ionic and neutral forms, corresponding to a certain pH value which was measured using pH-meter for each solution. The absorption maxima of the neutral and anionic forms of dyes are 530 and 680 nm (**3b**) and 515 and 645 nm (**4**), respectively.

#### 4.4. *Study of complexation*

The study of the complexation was realized as recommended in<sup>36</sup> using spectrophotometric titration according the limited logarithm Bent and French method<sup>30</sup> and the Molland method<sup>37</sup>. For this purpose, two series of solutions were prepared. The first series solutions contained equal amounts of  $\text{Zn}^{2+}$  (10  $\mu\text{mol}\cdot\text{L}^{-1}$  for **3b** and 5  $\mu\text{mol}\cdot\text{L}^{-1}$  for **4**), whereas the concentration of probe **3b** and **4** varied (10 - 90  $\mu\text{mol}\cdot\text{L}^{-1}$ ) and (0.5 - 81  $\mu\text{mol}\cdot\text{L}^{-1}$ ) respectively upon the adding the small portion of corresponding probe. The second series solutions contained equal amount of probe **3b** (38  $\mu\text{mol}\cdot\text{L}^{-1}$ ) or **4** (9.9  $\mu\text{mol}\cdot\text{L}^{-1}$ ), whereas the concentration of  $\text{Zn}^{2+}$  varied (2 - 90  $\mu\text{mol}\cdot\text{L}^{-1}$ ) and (1 - 112  $\mu\text{mol}\cdot\text{L}^{-1}$ ) respectively. The absorption spectra of these solutions were recorded and saturation curves  $\Delta A$

as the function of  $C$ ,  $\mu\text{mol}\cdot\text{L}^{-1}$  were obtained, where  $\Delta A = A_R - A_{ZnR}$  at the certain wavelength.

The molar composition of complexes ( $Zn_mR_n$ ) was established using the formula:  $n/m = (\Delta A_{\text{max}}^{Zn} \times C_R) / (\Delta A_{\text{max}}^R \times C_{Zn})$ , where  $m$  and  $n$  is the number of  $Zn^{2+}$  and the ligand attached to a metal ion consequently;  $\Delta A_{\text{max}}^{Zn}$  and  $\Delta A_{\text{max}}^R$  – absorption, corresponding to the saturation area;  $C_R$  and  $C_{Zn}$  – the initial concentrations of ligand and  $Zn^{2+}$  in solutions of each series.

The stability constants of the complexes were calculated using the Eq. 2:

$$K^f = \frac{\Delta A_i \cdot ([H^+] + K_a)}{(\Delta A_{\text{max}}^{Zn} - \Delta A_i) \cdot \left( C_R - n \frac{\Delta A_i}{\Delta A_{\text{max}}^{Zn}} C_{Zn} \right)^n \cdot [H^+]^{n(x-y)} \cdot (K_a)^n}, \quad (2)$$

where  $\Delta A_i$  is the value of absorbance in the initial linear section of the saturation curves;  $A_{\text{max}}^{Zn}$  is the value of absorbance in the saturation region;  $C_R$  is the concentration of probe, which corresponds to  $\Delta A_i$ ;  $C_{Zn}$  is the concentration of  $Zn^{2+}$ ;  $n$  is the number of coordinated ligands;  $x$  - number of protons capable of dissociation of dye **3b** or **4** ( $x = 1$ );  $y$  - number of protons detached from dye ( $y = 1$ );  $K_a$  - ionization constant of dye **3b** or **4**.

## 5. Acknowledgements

The authors acknowledge the generous support from the French Embassy in Kyiv, Ukraine, and Campus France for mobility allowance of O.K., the GDRI “Groupement Franco-Ukrainien en Chimie Moleculaire” for supporting such international collaboration, ANR for funding, and the CNRS, the Université de Toulouse, and the Taras Shevchenko National University of Kyiv for hosting our research. The authors acknowledge the scientific and technical support of the ICT services (<https://ict.cnrs.fr>) for NMR and HRMS analysis and Sonia Mallet-Ladeira for XRD analysis. The Enamine Ltd. company is acknowledged for providing the reagents.

## Associated content

Supporting information include NMR spectra for all the ligands, photostability test data, absorption properties data, deprotonation and complexation study data, and description of Zn<sup>2+</sup> detection in model solution of serum (pdf).

## Author information

Corresponding authors

Vladyslav V. Shcherban\*: schcherban@gmail.com

Tetiana Ye. Keda\*: tetianakeda@knu.ua

Co-authors

Olena O. Kuleshova: kuleshova.olena91@gmail.com

Olga V. Khilya: olga.v.khilya@gmail.com

Emmanuel Gras: emmanuel.gras@univ-tlse3.fr

Yulian M. Volovenko: yulian\_volovenko@ukr.net

## Autror Contriburions

The manuscript is written by the contribution of all authors. O.K. performed the synthesis and V.S. performed the compexation studies. All authors have given approval to the final version of the manuscript.

## References

---

(1) Wessels, I.; Maywald, M.; Rink, L. Zinc as a gatekeeper of immune function. *Nutrients* **2017**, *9*, 1286.

(2) Cunnane, S. Zinc clinical and biochemical significance, 1st ed.; CRC Press: Boca Raton, 2017.

(3) Pal, A.; Squitti, R.; Picozza, M.; Pawar, A.; Rongioletti, M.; Dutta, A.; Sahoo, S.; Goswami, K.; Sharma, P.; Prasad, R. Zinc and COVID-19: basis of current clinical trials. *Biol. Trace Elem. Res.* **2020**, *199*, 2882–2892.

(4) Name, J.; Souza, A.; Vasconcelos, A.; Prado, P.; Pereira, C. Zinc, vitamin D and vitamin C: perspectives for COVID-19 with a focus on physical tissue barrier integrity. *Front. nutr.* **2020**, *7*.

- 
- (5) Wessels, I.; Rolles, B.; Rink, L. The potential impact of zinc supplementation on COVID-19 pathogenesis. *Front. Immunol.* **2020**, *11*.
- (6) Jampilek, J.; Kralova, K. Potential of nanonutraceuticals in increasing immunity. *Nanomaterials* **2020**, *10*, 2224.
- (7) Skalny, A.; Aschner, M.; Tinkov, A. Chapter eight - zinc. In *Advances in food and nutrition research*, 2021; pp 251–310.
- (8) Benoist, B.; Darnton-Hill, I.; Davidsson, L.; Fontaine, O.; Hotz, C. Conclusions of the joint WHO/UNICEF/IAEA/izincg interagency meeting on zinc status indicators. *Food Nutr. Bull. Suppl.* **2007**, *28*, S480–S484.
- (9) Wieringa, F.; Dijkhuizen, M.; Fiorentino, M.; Lailou, A.; Berger, J. Determination of zinc status in humans: which indicator should we use?. *Nutrients* **2015**, *7*, 3252–3263.
- (10) King, J.; Brown, K.; Gibson, R.; Krebs, N.; Lowe, N.; Siekmann, J.; Raiten, D. Biomarkers of nutrition for development (BOND)—Zinc Review. *J. Nutr.* **2015**, *146* (4), 858S–885S.
- (11) Planeta, K.; Kubala-Kukus, A.; Drozd, A.; Matusiak, K.; Setkowicz, Z.; Chwiej, J. The assessment of the usability of selected instrumental techniques for the elemental analysis of biomedical samples. *Sci. Rep.* **2021**, *11*.
- (12) Hall, A.; King, J.; McDonald, C. comparison of serum, plasma, and liver zinc measurements by AAS, ICP-OES, and ICP-MS in diverse laboratory settings. *Biol. Trace Elem. Res.* **2021**, *200*, 2606–2613.
- (13) Diana, R.; Panunzi, B. Zinc(II) and aiegens: the “clip approach” for a novel fluorophore family. A review. *Molecules* **2021**, *26*, 4176.
- (14) Marczenko, Z.; Balcerzak, M. Chapter 56 - Zinc. In *Analytical spectroscopy library*, 2000; pp 466–473.
- (15) Kocyla, A.; Pomorski, A.; Krężel, A. Molar absorption coefficients and stability constants of metal complexes of 4-(2-pyridylazo)resorcinol (PAR): revisiting common chelating probe for the study of metalloproteins. *J. Inorg. Biochem.* **2015**, *152*, 82–92.
- (16) Kocyla, A.; Pomorski, A.; Krężel, A. Molar absorption coefficients and stability constants of zincon metal complexes for determination of metal ions and bioinorganic applications. *J. Inorg. Biochem.* **2017**, *176*, 53–65.
- (17) Makino, T. A Sensitive, direct colorimetric assay of serum zinc using nitro-PAPS And Microwell Plates. *Clin. Chim. Acta* **1991**, *197*, 209–220.
- (18) Qi, Z.; Cheng, Y.; Xu, Z.; Chen, M. Recent advances in porphyrin-based materials for metal ions detection. *Int. J. Mol. Sci.* **2020**, *21*, 5839.
- (19) Zajun, L.; Jiaomai, P. Advances in synthesis and application of the derivatives of porphyrin as reagents in analytical chemistry. *Rev. Anal. Chem.* **2002**, *21*, 167–231.
- (20) Paolesse, R.; Nardis, S.; Monti, D.; Stefanelli, M.; Di Natale, C. Porphyrinoids for chemical sensor applications. *Chem. Rev.* **2016**, *117*, 2517–2583.

---

(21) Negut, C.; Stefan - van Staden, R.; van Staden, J. Porphyrins - as active materials in the design of sensors. An overview. *ECS J. Solid State Sci. Technol.* **2020**, *9*, 051005.

(22) Ding, Y.; Tang, Y.; Zhu, W.; Xie, Y. Fluorescent and colorimetric ion probes based on conjugated oligopyrroles. *Chem. Soc. Rev.* **2015**, *44*, 1101–1112.

(23) Senge, M.; Sergeeva, N.; Hale, K. Classic highlights in porphyrin and porphyrinoid total synthesis and biosynthesis. *Chem. Soc. Rev.* **2021**, *50*, 4730–4789.

(24) Cornforth, J.; Hitchcock, P.; Rozos, P. Isatin chloride: a phantom. reactions of 2-(2,2-dichloro-2,3-dihydro-3-oxoindol-1-yl)-3H-indol-3-one. *J. Chem. Soc., Perkin Trans. 1* **1996**, *23*, 2787–2792.

(25) Katritzky, A.; Fan, W.; Koziol, A.; Palenik, G. 2-chloro-3H-indol-3-one and its reactions with nucleophiles. *J. Heterocycl. Chem.* **1989**, *26*, 821–828.

(26) Campagna, F.; Palluotto, F.; Mascia, M.; Maciocco, E.; Marra, C.; Carotti, A.; Carrieri, A. Synthesis and biological evaluation of pyridazino[4,3-b]indoles and indeno[1,2-c]pyridazines as new ligands of central and peripheral benzodiazepine receptors. *Il Farmaco* **2003**, *58*, 129–140.

(27) Kuleshova, O.; Shcherban, V.; Khilya, O.; Keda, T.; Zaporozhets, Z.; Volovenko, Y. 2-Hetaryl-2-(5-R-3-oxoindolin-2-ylidene)acetonitriles, method of their synthesis and application for spectrophotometric 3d-metals determination. 120127, 2019.

(28) Kuleshova, O.; Khilya, O.; Volovenko, Y. New method for the synthesis of 2-hetaryl-2-(1-R-pyrrolidin-2-ylidene)acetonitriles. *Chem. Heterocycl. Compd.* **2018**, *54*, 83–85.

(29) Kovalska, N.; Kariaka, N.; Litsis, O.; Kuleshova, O.; Khilya, O.; Slyva, T.; Amirkhanov, V. Spectral properties of transition metal coordination compounds with heterocyclic enamionitriles. *Bulletin of Taras Shevchenko National university of Kyiv, Chemistry* **2015**, *1*, 16–19.

(30) Bent, H.; French, C. The structure of ferric thiocyanate and its dissociation in aqueous solution. *J. Am. Chem. Soc.* **1941**, *63*, 568–572

(31) Baranyai, E.; Tóth, C.; Fábíán, I. Elemental analysis of human blood serum by microwave plasma—investigation of the matrix effects caused by sodium using model solutions. *Biol. Trace Elem. Res.* **2019**, *194*, 13–23.

(32) Kuleshova, O. Cyclic 2-azahetaryl-3-enaminonitriles: toward synthesis of functionalized azaheterocycles, metal complexation and probes design. Ph.D. Dissertation, Université Paul Sabatier - Toulouse III, 2018. <http://thesesups.ups-tlse.fr/4036/1/2018TOU30127.pdf> <https://tel.archives-ouvertes.fr/tel-02130482/document> (accessed 2019-05-15).

(33) Kuleshova, O.; Khilya, O.; Volovenko, Yu.; Mallet-Ladeira, S.; Dyakonenko, V.; Gras, E. Expedited route to fully substituted amino-pyrazole building blocks and their further transformations. *ACS Omega* **2017**, *2*, 8911–8927.

( 34 ) McCall, J. M.; Ursprung, J, J. The upjohn company. N,2-dicyanoacetimidates. US 4 032 559 A1, 1977.

(35) Albert, A.; Serjeant, E. The determination of ionization constants, 3<sup>rd</sup> ed.; Springer: Dordrecht, 1984; pp 70-75.

(36) Zaporozhets, O.; Paustovska, A.; Zinko, L.; Davydov, V. Formation of the intensively fluorescent mixed-ligand complex of  $Zr(OH)^{3+}$  with 3,5,7,2',4'-pentahydroxyflavone in the presence of fluoride. *J. Fluorine Chem.* **2015**, *170*, 52-56.

(37) Molland, J. Inner complex salts of the 8-hydroxyquinoline-5-sulfonic acid. *J. Am. Chem. Soc.* **1940**, *62*, 541-542.

